Available online at www.sciencedirect.com
SCIENCE DIRECT
Biochemical and Biophysical Research Communications 340 (2006) 151–157
BBRC
www.elsevier.com/locate/ybbrc

The refractory periods and threshold potentials of sequential spikes measured by whole-cell recording ☆

Na Chen [a,b], Shuli Chen [a], Yingliang Wu [b], Jinhui Wang [a,*]

[a] State Key Laboratory for Brain and Cognitive Sciences, National Laboratory for Protein Sciences, Institute of Biophysics Chinese Academy of Sciences, Beijing 100101, China

[b] The Department of Pharmacology, The College of Pharmacy, Shenyang Pharmaceutical University, Shenyang, Liaoning 110016, China

Received 21 November 2005
Available online 9 December 2005

Abstract

Neurons in the central nervous system are thought to program neural language via firing sequential spikes for guiding animal behaviors. The quantitative profiles of spike intrinsic properties are critically important to understand spike programming. We developed approaches with whole-cell recordings to measure the threshold potentials and refractory periods (RPs) of *sequential spikes*, and to analyze the relationships of these factors with spike timing precision and capacity at the regular-spiking and fast-spiking neurons in cortical slice. The RPs and threshold potentials of sequential spikes at these two groups of neurons are different and are linearly correlated with spike timing precision and capacity. These data suggest that RPs and threshold potentials essentially navigate the spike programming for the precise and loyal encoding of meaningful neural signals. Our study provides the avenues for decoding the spectrum of the neural signals quantitatively.

Keywords: Action potential; Spike timing precision; Spike capacity; Refractory period; Threshold potential and cortical neuron

Human behaviors are performed precisely under physiological conditions, which are guided by a set of neural languages (the spectrum of neural signals) programmed at neurons and synapses in the brain. The molecular mechanisms underlying neural behaviors were investigated extensively [1,2], however, it is poorly understood how neurons, accommodating the network of molecules, integrate hundreds of presynaptic inputs and encode spike patterns that constitute the neural languages [3]. The lag in decoding neuronal signals is likely due to lack of approaches to quantify the properties, such as refractory periods (RPs) and threshold potentials, of sequential spikes.

In the programming of neural signals, spike patterns (e.g., adaptable sequential spikes or tonic spike bursts) and inter-spike intervals, likely silicon-based switch, are the preferred candidate of neural computational processes [4–6]. Spike timing precision is also critical [7,8] since precise and loyal spike patterns symbolize neuronal events in the meaningful and memorable manner. In terms of mechanisms underlying spike programs, synaptic plasticity [9–12] and potassium channel-mediated after-hyperpolarization [13–20] are thought to be involved. However, spike intrinsic properties, such as the threshold potentials and RPs, should be essential for generating the patterns of sequential spikes. Little, if any, studies were done to quantify the RPs and threshold potentials of *sequential spikes*, and to address how these factors manage the programming of neuronal signals.

To the questions above, we paid attention to quantifying the threshold potentials and RPs of sequential spikes, and to addressing the role of these factors in setting spike capacity and timing precision at regular- and fast-spiking

☆ *Abbreviations:* V_r, resting membrane potential; V_{ts}, threshold potential; $V_{ts} - V_r$, the difference between threshold potential and resting membrane potential; RP, refractory period; RSN, regular-spiking neuron; FSN, fast-spiking neuron; ISI, inter-spike interval; SDST, standard deviation of spike timing.

* Corresponding author.
E-mail address: jhw@sun5.ibp.ac.cn (J. Wang).

0006-291X/$ - see front matter © 2005 Elsevier Inc. All rights reserved.
doi:10.1016/j.bbrc.2005.11.170

neurons by whole-cell recordings in cortical slices. The RPs and threshold potentials are essential to navigating spike capacity and timing precision at cortical regular- and fast-spiking neurons. Our studies provide avenues to elucidate the precise analyses and computation of neural signals quantitatively in the central nervous system.

Methods and materials

Brain slices. Cortical slices (400 μm) were prepared from Sprague–Dawley rats (postnatal day 16–22) that were anesthetized by injecting pentobarbital (50 mg/kg) and decapitated with a guillotine. The slices were cut with a Vibratome in the modified and oxygenized (95% O_2/5% CO_2) artificial cerebrospinal fluid (mM: 124 NaCl, 3 KCl, 1.2 NaH_2PO_4, 26 $NaHCO_3$, 0.5 $CaCl_2$, 5 $MgSO_4$, 10 dextrose, and 5 Hepes, pH 7.35) at 4 °C, and then were held in the normal oxygenated ACSF (mM: 124 NaCl, 3 KCl, 1.2 NaH_2PO_4, 26 $NaHCO_3$, 2.4 $CaCl_2$, 1.3 $MgSO_4$, 10 dextrose, and 5 Hepes, pH 7.35) at 24 °C for 1–2 h before experiments. A slice was transferred to the submersion chamber (Warner RC-26G) that was perfused with the normal ACSF at 31 °C for the whole-cell recordings [21]. Chemicals were purchased from Fisher Scientific. The procedures were approved by IACUC in Beijing, China.

Neuron selection. Neurons in layer II–III of sensorimotor cortex were recorded. Regular-spiking neurons (RSN) show pyramidal-like soma and an apical dendrite; and fast-spiking neurons (FSN) are round with multipolar processes under DIC optics (Nikon FN-E600). RSN and FSN show the different properties in the response to the hyperpolarization and depolarization pulses [21–23], especially spike patterns (Figs. 1 and 2).

Whole-cell recording. Electrical signals at the cortical neurons were recorded with Axoclamp-2B or multi-clamp 700B Amplifiers (Axon Instrument, Foster CA, USA) in current clamp model and inputted into pClamp 9 (Axon Instrument) for the data acquisition and analyses. The output bandwidth of amplifiers was set at 3 kHz. The input resistance was monitored by injecting hyperpolarization pulses throughout each of experiments to be sure recording quality. The spike patterns and intrinsic properties at regular-spiking and fast-spiking neurons were studied by applying depolarization current pulses.

The standard pipette solution contains (mM) 150 K-gluconate, 5 NaCl, 10 Hepes, 0.4 EGTA, 4 Mg-ATP, 0.5 Tris–GTP, and 4 Na-phosphocreatine (pH 7.4 adjusted by 2 M KOH). Fresh pipette solution was filtered with the 0.1 μm centrifuge filter before use. The osmolarity of pipette solution was 295–305 mOsmol and resistance was 6–8 MΩ.

The measurement and analysis of neuronal intrinsic properties. Neuronal intrinsic properties in our studies include the threshold potentials of firing sequential spikes, the RPs subsequent to each of spikes, as well as the output patterns of spike programming (inter-spike intervals and the standard deviation of spike timing).

The thresholds of sequential spikes were measured based on the differences between resting membrane potential (V_r) and threshold potentials (V_{ts}), at which the rising phase of spikes (e.g., spikes 1–5) starts represents an energy barrier for how easily spikes are evoked, which is an index of neuronal intrinsic properties. RPs subsequent to action potentials at cortical neurons were measured by intracellularly injecting depolarization-current pulses (3 ms) after each of spikes (see Fig. 3). Through changing inter-pulse intervals, we defined absolute RP as a duration from a complete spike to a subsequent spike at 50% of firing probability, and relative RP as a duration from a complete spike to a subsequent spike that fires 100% of probability and initially reaches the amplitudes of natural spikes.

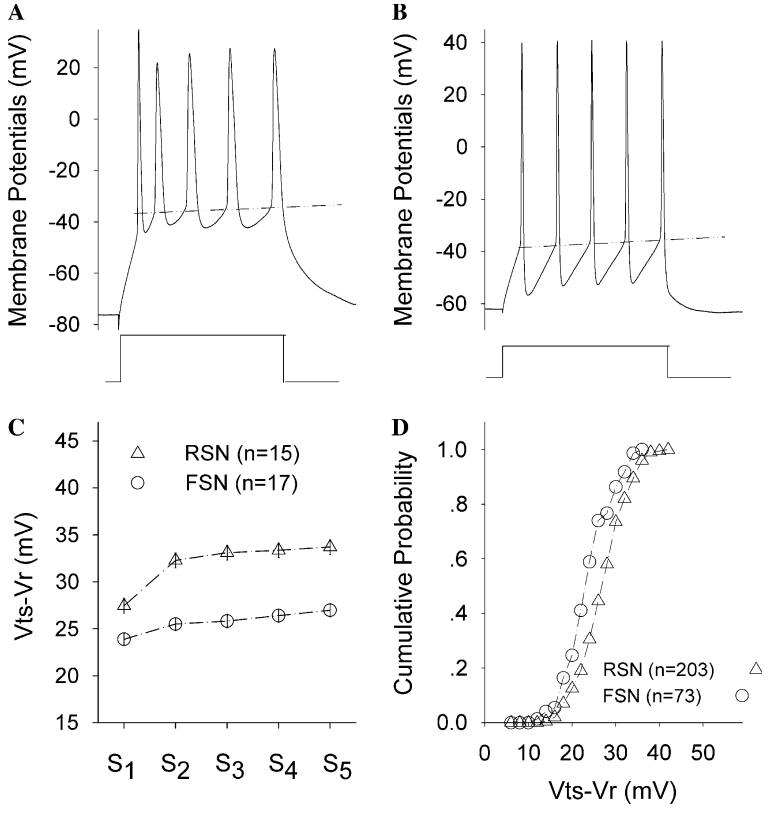

Fig. 1. The quantitative measurements of threshold potentials of sequential spikes by whole-cell current clamp recordings in cortical RSN and FSN. (A,B) The ways are used to measure the threshold potentials of firing five sequential spikes (V_{ts}, dot-dash line) at RSN (A) and FSN (B). (C) The values and the comparison of threshold potentials ($V_{ts} - V_r$) of spikes 1–5 at RSN (triangle) and FSN (circles). (D) A comparison of cumulative probability of $V_{ts} - V_r$ at RSN (triangles) and FSN (circles).

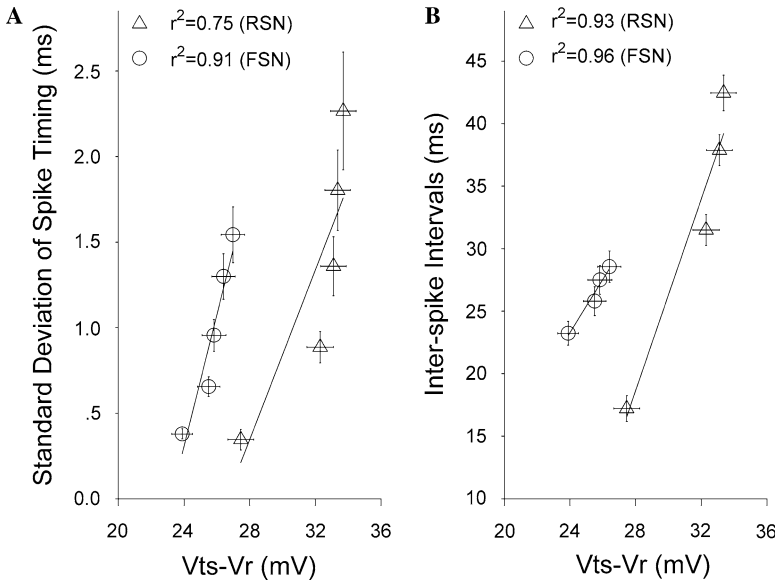

Fig. 2. The relationships between threshold potentials and SDST or ISI in cortical RSN (triangles) and FSN (circles). (A) A linear correlation between $V_{ts} - V_r$ and SDST at RSN ($r^2 = 0.75$) and FSN ($r^2 = 0.91$). (B) A linear correlation between $V_{ts} - V_r$ and ISI at RSN ($r^2 = 0.93$) and FSN ($r^2 = 0.96$).

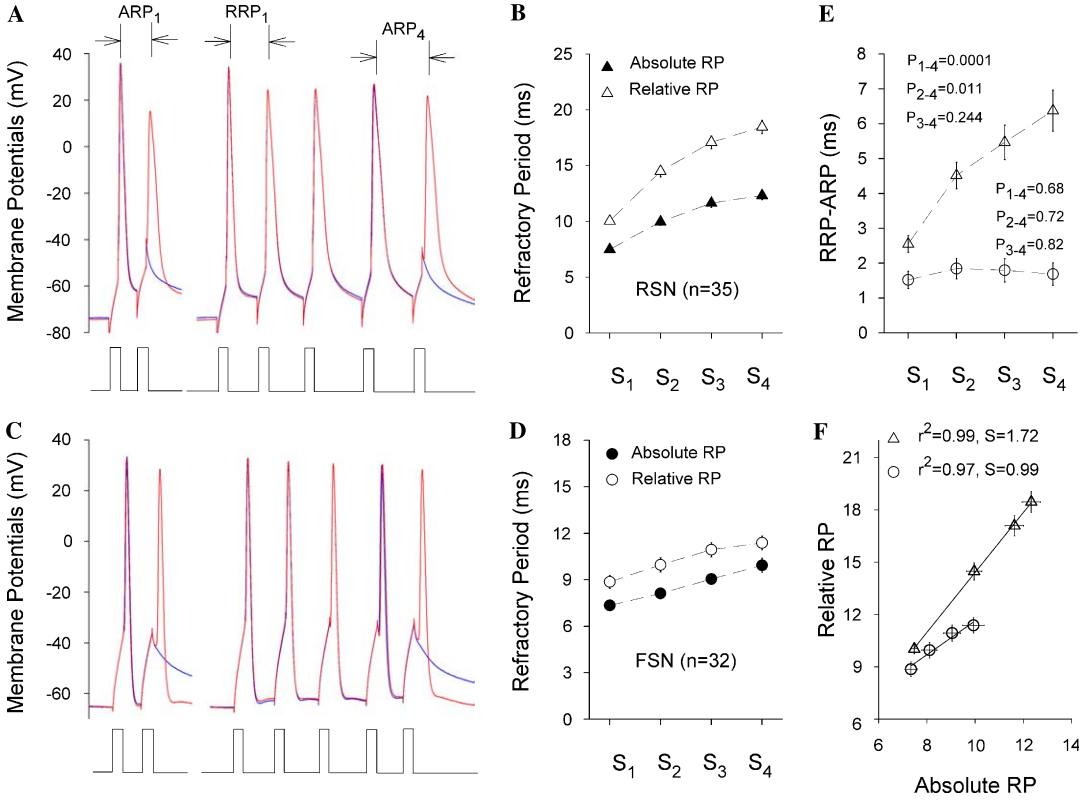

Fig. 3. The measures of the RP subsequent to each of spikes in cortical RSN (triangles, A and B) and FSN (circles, C and D). (A) The methods are used to measure absolute RP and relative RP at RSN. ARP is defined as the duration from a complete spike to a subsequent spike at 50% of probability; and RRP as the duration from a complete spike to a subsequent spike with 100% of probability as well as the amplitude initially reached natural spikes. (B) Quantitative data show ARP (filled triangles) and RRP (open triangles) subsequent to spikes (S) 1–4 at RSN ($n = 35$). (C) The methods are used to measure ARP and RRP at FSN. (D) Quantitative data show ARP (filled circles) and RRP (open circles) subsequent to spikes (S) 1–4 at FSN ($n = 32$). (E) The difference between RRP and ARP subsequent to spikes 1–4. The comparisons from spikes 1–4, 2–4 to 3–4 are given ($p_{1-4} = 0.0001$, $p_{2-4} = 0.011$, and $p_{3-4} = 0.24$, triangles) at RSN. The difference between RRP and ARP after spikes 1–4 and the comparisons from spikes 1–4, 2–4 to 3–4 are given ($p_{1-4} = 0.68$, $p_{2-4} = 0.72$, and $p_{2-4} = 0.82$, circles) at FSN. (F) The correlations between RRP and ARP subsequent to spikes 1–4 are linear at RSN ($r^2 = 0.99$, slope = 1.72, triangles) and FSN ($r^2 = 0.97$, slope = 0.99, circles).

Inter-spike intervals (ISI, an index of spike capacity) and the standard deviation of spike timing (SDST, an index of spike precision) were analyzed by evoking repetitive spikes with depolarization currents (>100 ms). ISI is the duration between spike pairs; and SDST is a standard deviation of spike lock phase.

Data were analyzed if V_r was above −60 mV at the recorded fast-spiking neurons and −67 mV at regular-spiking cells. The criteria for the acceptance of each experiment also included less than 5% changes in V_r, spike magnitude, and input resistance throughout each of experiments. The values of spike threshold, RP, ISI, and SDST are presented as means ± SE. Comparisons under different conditions were done by *t* test.

Results

Spike capacity and timing precision are hypothetically set by interactions between synaptic inputs and the neuronal intrinsic property. To address how neuronal intrinsic properties influence spike programming, we developed approaches to measure the threshold potentials and RPs of sequential spikes, as well as their role in navigating spike capacity and timing precision at regular-spiking neurons (RSN) and fast-spiking neurons (FSN) by whole-cell recording in cortical slices.

The threshold potentials of sequential spikes at RSN and FSN

Threshold stimuli by extracellular stimulus [24] or intracellular current injections [25–28] are used to merit neuronal excitability, which represents a minimal intensity of *extrinsic* excitatory inputs to fire spikes. In addition to a single value of threshold stimuli for sequential spikes, the efficiency of current injections will be deteriorated by the variation of input resistance among neurons, which causes the huge diversified threshold stimuli (our unpublished data). We applied the differences between threshold potential (V_{ts}) and resting membrane potential (V_r) as a neuronal *intrinsic* property to present the firing of spikes.

Fig. 1 illustrates the measurements and values of threshold potentials for the sequential spikes, which are defined as the points of membrane potentials, at which the rapid rising phase of action potentials starts. The sequential spikes, evoked by a depolarization pulse, are shown in Fig. 1A at RSN and Fig. 1B at FSN, in which the dash lines indicate the threshold potentials. The values of $V_{ts} - V_r$ for spikes 1–5 are 27.46 ± 0.79, 32.3 ± 0.8, 33.1 ± 0.78, 33.36 ± 0.77, and 33.71 ± 0.77 mV at RSN (triangles in Fig. 1C). The values of $V_{ts} - V_r$ for spikes 1–5 are 23.89 ± 0.63, 25.5 ± 0.68, 25.83 ± 0.73, 26.4 ± 0.7, and 26.98 ± 0.7 mV at FSN (circles in Fig. 1C). The $V_{ts} - V_r$ values relevant to the same number in the sequence of spikes are significantly lower at FSN than RSN ($p < 0.01$). Lower threshold potentials at FSN support a notion that FSNs are highly excitable [22,29,30], i.e., more sensitive to excitatory inputs, compared to RSN.

Noteworthy, by analyzing the cumulative probability of threshold potential at RSN and FSN, we found that the values of $V_{ts} - V_r$ vary among 20–35 mV, in addition to the differences in their values (Fig. 1D). This result indicates that neurons in the cerebral cortex express the different sensitivities to extrinsic inputs to be excited.

The threshold potentials navigate spike programming

In order to clarify the role of threshold potentials in the programming of sequential spikes, we investigated the relationship between $V_{ts} - V_r$ and spike timing precision or capacity. The spike timing precision is represented by the standard deviation of spike timing (SDST), which is calculated from 50 traces of sequential spikes. Spike capacity is expressed by the inter-spike intervals (ISI) of sequential spikes, which are averaged from 50 traces.

The values of $SDST_1$ to $SDST_5$ are 0.35 ± 0.06, 0.89 ± 0.09, 1.36 ± 0.17, 1.8 ± 0.24, and 2.27 ± 0.34 ms at RSN; and the values are 0.39 ± 0.03, 0.66 ± 0.06, 0.96 ± 0.094, 1.3 ± 0.13, and 1.54 ± 0.16 ms at FSN. To the inter-spike intervals, the values of ISI_1 to ISI_4 are 17.21 ± 1.04, 31.5 ± 1.24, 37.88 ± 1.23, and 42.46 ± 1.42 ms at RSN; and the value are 23.23 ± 0.95, 25.8 ± 1.15, 27.5 ± 1.15. and 28.56 ± 1.26 ms at FSN. Moreover, the values of $V_{ts} - V_r$ for spikes 1–5 are 27.46 ± 0.79, 32.3 ± 0.8, 33.1 ± 0.78, 33.36 ± 0.77, and 33.71 ± 0.77 at RSN; and the values are 23.89 ± 0.63, 25.5 ± 0.68, 25.83 ± 0.73, 26.4 ± 0.7, and 26.98 ± 0.71 mV at FSN, respectively.

We plotted the relationship between $V_{ts} - V_r$ and SDST or ISI in figure two. The correlations between $V_{ts} - V_{r1-5}$ and $SDST_{1-5}$ appear linear at FSN ($r^2 = 0.91$, circles in Fig. 2A) and at RSN ($r^2 = 0.75$, triangles). The correlations between $V_{ts} - V_{r1-5}$ and ISI (ISI_{1-2} through ISI_{4-5}) are linear at FSN ($r^2 = 0.96$, circles in Fig. 2B) and at RSN ($r^2 = 0.93$, triangles). The data indicate that threshold potentials essentially control spike timing precision and capacity.

The refractory periods of sequential spikes at RSN and FSN

The values of ISI in sequential spikes at RSN increase gradually, whereas ISI at FSN is close to one another (Figs. 1 and 2). In addition to the role of $V_{ts} - V_r$, RP subsequent to each of spikes may be another factor to control ISI, in turn spike capacity. If it is a case, RP should be correlated with ISI. We developed an approach to quantify the absolute and relative RP of sequential spikes by injecting depolarization pulses (3 ms) following each of spikes into the recorded neurons. With changing inter-pulse intervals, we defined absolute RP as the duration from a complete spike to a subsequent spike at 50% of firing probability, and relative RP as the duration from a complete spike to a subsequent spike that fires 100% of probability and initially reaches the amplitudes of natural spikes (Figs. 3A and C).

Figs. 3B and D present the quantitative data at RSN and FSN. ARP values of spikes 1–4 are 7.48 ± 0.16, 9.97 ± 0.32, 11.63 ± 0.39, and 12.3 ± 0.4 ms (filled trian-

gles in Fig. 3B); and RRP values for spikes 1–4 are 10.03 ± 0.28, 14.48 ± 0.5, 17.1 ± 0.59, and 18.46 ± 0.61 ms at RSN (opened triangles in Fig. 3B; $n = 35$). In FSN, ARP values of spikes 1–4 are 7.33 ± 0.27, 8.11 ± 0.3, 9.1 ± 0.35, and 9.9 ± 0.46 ms (filled circles, Fig. 3D); and RRP values for spikes 1–4 are 8.86 ± 0.42, 9.96 ± 0.45, 10.93 ± 0.47, and 11.38 ± 0.44 ms ($n = 32$, opened circles in Fig. 3D). Increases in the RPs of sequential spikes at RSN may cause inter-spike intervals to be gradually prolonged and less increase in RPs at FSN may explain "equal" inter-spike intervals.

Interestingly, the differences between RRP and ARP ($\triangle$RP) from spike 1 to spike 4 are 2.55 ± 0.24, 4.52 ± 0.38, 5.47 ± 0.5, and 6.38 ± 0.6 ms at RSN (triangles in Fig. 3E), where $p_{1-2} = 0.001$, $p_{2-4} = 0.01$, and $p_{3-4} = 0.24$, respectively. In FSN, $\triangle$RP for spikes from 1 to 4 are 1.52 ± 0.24, 1.84 ± 0.3, 1.79 ± 0.34, and 1.68 ± 0.32 ms (circles in 3E), in which $p_{1-2} = 0.68$, $p_{2-4} = 0.72$, and $p_{3-4} = 0.8$. Moreover, Fig. 3F demonstrates that ARP and RRP are linearly correlated at RSN ($r^2 = 0.99$, slope is 1.72; triangles) and FSN ($r^2 = 0.97$, the slope is 0.99; circles in Fig. 3F). Although a linear correlation between ARP and RRP denotes same mechanisms underlying ARP and RRP values, a gradual increase in $\triangle$RP and larger than one of their linear slope imply an unparallel change in ARP and RRP of sequential spikes at cortical RSN, which further implies that ARP and RRP are controlled by two dynamic processes.

The refractory periods navigate spike programming

We examined the role of RPs in controlling spike programming by plotting the relationship between the RPs and inter-spike interval (spike capacity, Fig. 4A) or the standard deviation of spike timing (spike precision, Fig. 4B). ARP and ISI are linearly correlated at RSN (triangles, $r^2 = 0.99$) and FSN (circles, $r^2 = 0.91$). Similarly, ARP and SDST are linearly correlated at RSN (triangles, $r^2 = 0.99$) and FSN (circles, $r^2 = 0.99$). Such results indicate that RPs subsequent to each of spikes are important factor controlling spike capacity and timing precision.

Discussion

By quantifying the RP and threshold potential of *sequential spikes*, we studied their role in spike capacity and timing precision. The threshold potentials and RPs of sequential spikes are lower at fast-spiking cells; and the linear correlations between threshold potentials and spike timing precision or capacity are better at fast-spiking than regular-spiking neurons. Such differences in neuronal intrinsic property well explain why fast-spiking cells are more sensitive to excitatory inputs [31] and express a higher capacity in spike programming. Moreover, RPs are linearly correlated with spike capacity and timing precision; and the threshold potentials are linearly correlated with RPs. These data indicate that spike capacity and timing precision at cortical neurons are under the control of spike intrinsic properties, which help us to understand the principles from neuronal intrinsic property to neural signal encodings.

Spike thresholds and the extended considerations

We quantified the *intrinsic* threshold potentials for sequential spikes. Their values in sequential spikes keep away from resting membrane potential, especially between spikes 1 and 2–5 at regular-spiking cells (Fig. 1). If the kinetics of voltage-gated sodium channels underlie threshold potentials [24,32–34], each of sodium channels or some of them on cell membrane may not be completely recovered

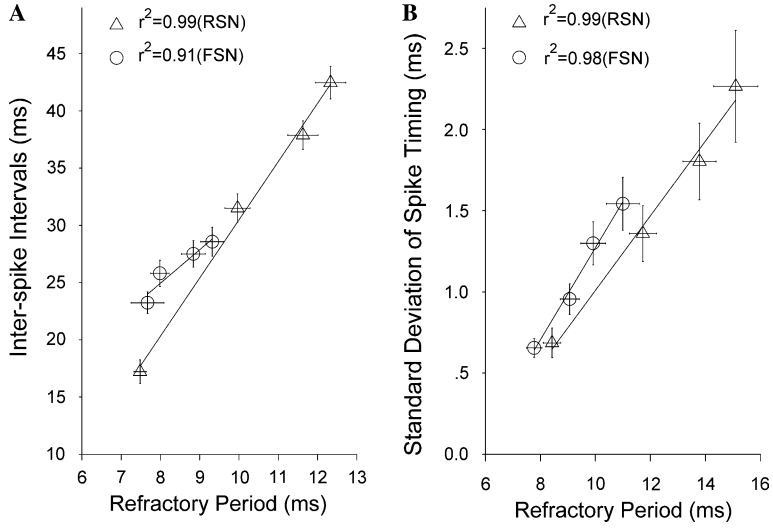

Fig. 4. The relationships between RPs and SDST or ISI in cortical RSN (triangles) and FSN (circles). (A) The linear correlations between ARP and ISI at RSN ($r^2 = 0.99$, triangles) or FSN ($r^2 = 0.91$, circles). (B) The linear correlations between ARP and SDST at RSN ($r^2 = 0.99$, triangles) or FSN ($r^2 = 0.98$, circles).

from their inactivation when firing subsequent spikes though their RPs are over. In this regard, the threshold potentials may more sensitively reflect the kinetics of sodium channels.

In terms of physiological roles of threshold potentials, we found that the threshold potentials of sequential spikes are linearly correlated with inter-spike intervals and the standard deviation of spike timing, indicating that this parameter is involved in ruling spike capacity and timing precision. It is noteworthy that threshold potentials vary among cortical neurons. The diversified sensitivity of cortical neurons to synaptic inputs grants the neurons in networks having a range of abilities in encoding spikes. If a network is responsible for a behavior in animals, the language from this network would be encoded by a group of neurons that sing the different rhythms.

Refractory periods and their role in spike capacity and precision

We developed an approach to measure the RPs of sequential spikes with whole-cell recordings. Our results show that the RPs of sequential spikes are prolonged at regular-spiking cells that show an increased inter-spike intervals in multiple spikes; whereas RPs are less changed, similar to ISI, at fast-spiking neurons. Together with the facts that the RPs are linearly correlated with both inter-spike intervals and the standard deviation of spike timing, we suggest that the RPs subsequent to each of spikes, similar to threshold potentials, rule spike capacity and timing precision at cortical regular- and fast-spiking neurons.

In addition to a difference of RPs at regular-spiking and fast-spiking neurons, the differences between RRP and ARP ($\triangle$RP) of spikes 1–4 are statistically different at RSN (Fig. 3E). ARP and RRP are linearly correlated; and the slopes of lines are 1.72 at RSN and 0.99 at FSN (Fig. 3F). These data imply that the mechanisms underlying RPs are different at RSN and FSN, which may be due to the differences in the kinetics of voltage-gated sodium channels. A gradual increase in $\triangle$RP and larger than one in linear slope between ARP and RRP imply that ARP and RRP are controlled by two dynamic processes at RSN.

With our developed approaches to quantify the threshold potentials and RPs of sequential spikes, which voltage-gated sodium channels underlie [24], we found that they are essentially navigating spike capacity and timing precision at cortical regular-spiking and fast-spiking neurons. Our data emphasize the role of the threshold potentials and RPs in spike programming, besides synaptic plasticity [9–12] and potassium channel-mediated after-hyperpolarization [14–20]. Furthermore, our studies link the knowledge between the kinetics of VGSC and the encoding of neural signals, as well as provide avenues for addressing the precise analyses and computation of neural signals quantitatively in the brain.

Acknowledgments

J.H. Wang initiates and designs this study. The study is supported by National Awards for Outstanding Young Scientist (30325021), Natural Science Foundation of China (30470362), Program for Hundred Talent and Gifted Scientist by Chinese Academy of Sciences, and National Basic Research Program (2006CB500804) to J.H.W.

References

[1] A.V. Anagnostopoulos, L.E. Mobraaten, J.J. Sharp, M.T. Davisson, Transgenic and knockout databases: behavioral profiles of mouse mutants, Physiol. Behav. 73 (2001) 675–689.
[2] G. Horn, Pathways of the past: the imprint of memory, Nat. Rev. Neurosci. 5 (2004) 108–120.
[3] S. Grillner, H. Markram, E.D. Schutter, G. Silberger, F.E.N. LeBeau, Microcircuits in action—from CPGs to neocortex, Trends Neurosci. 28 (2005) 525–533.
[4] M. London, A. Schreibman, M. Hausser, M.E. Larkum, I. Segev, The information efficacy of a synapse, Nat. Neurosci. 5 (2002) 332–340.
[5] M.N. Shadlen, W.T. Newsome, Noise, neural codes and cortical organization, Curr. Opin. Neurobiol. 4 (1994) 569–579.
[6] P.H.E. Tiesinga, J.V. Toups, The possible role of spike patterns in cortical information processing, J. Comput. Neurosci. 18 (2005) 275–286.
[7] D. Fricker, R. Miles, Interneuron, spike timing, and perception, Neuron 32 (2001) 771–774.
[8] R.S. Petersen, S. Panzeri, M.E. Diamond, Population coding in somatosensory cortex, Curr. Opin. Neurobiol. 12 (2002) 441–447.
[9] D. Daoudal, D. Debanne, Long-term plasticity of intrinsic excitability: learning rules and mechanisms, Learn. Mem. 10 (2003) 456–465.
[10] P. Somogyi, T. Klausberger, Defined types of cortical interneuron structure space and spike timing in the hippocampus, J. Physiol. (Lond.) 562 (2005) 9–29.
[11] N.C. Spitzer, P.A. Kingston, T.J. Manning Jr., M.W. Conklin, Outside and in: development of neuronal excitability, Curr. Opin. Neurobiol. 12 (2002) 315–323.
[12] W. Zhang, D. Linden, The other side of the engram: experience-driven changes in neuronal intrinsic excitability, Nat. Rev. Neurosci. 4 (2003) 885–900.
[13] P.A. Glazebrook et al., Potassium channels Kv1.1, Kv1.2 and Kv1.6 influence excitatory of rat visceral sensory neurons, J. Physiol. (Lond.) 541 (2002) 467–482.
[14] D. Hess, A.E. Manira, Characterization of a high-voltage-activated Ia current with a role in spike timing and locomotor pattern generation, Proc. Natl. Acad. Sci. USA 98 (2001) 5276–5281.
[15] D. Johnston et al., Dendritic potassium channels in hippocampal pyramidal neurons, J. Physiol. (Lond.) 525 (2000) 75–81.
[16] J. Kang, J.R. Huguenard, D. Prince, Voltage-gated potassium channels activated during action potentials in layer V neocortical pyramidal neurons, J. Neurophysiol. 83 (2000) 70–80.
[17] S. Nedergarrd, Regulation of action potential size and excitability in substantia nigra compacta neurons: Sensitivity to 4-aminopyridine, J. Neurophysiol. 82 (1999) 2903–2913.
[18] B. Rudy et al., Contributions of Kv3 channels to neuronal excitability, Ann. N. Y. Acad. Sci. 868 (1999) 304–343.
[19] P. Sah, Ca.2+-activated K+ currents in neurones: types, physiological roles and modulation, Trends Neurosci. 19 (1996) 150–154.
[20] M. Wehr, A.M. Zador, Balanced inhibition underlies tuning and sharpens spike timing in auditory cortex, Nature 426 (2003) 442–446.
[21] J.-H. Wang, Short-term cerebral ischemia causes the dysfunction of interneurons and more excitation of pyramidal neurons, Brain Res. Bull. 60 (2003) 53–58.

[22] B.W. Connors, M.J. Gutnick, Intrinsic firing patterns of diverse neocortical neurons, Trends Neurosci. 13 (1990) 99–104.
[23] J.-H. Wang, P.T. Kelly, Ca2+/CaM signalling pathway up-regulates glutamatergic synaptic function in non-pyramidal fast-spiking neurons of hippocampal CA1, J. Physiol. (Lond.) 533 (2001) 407–422.
[24] M.C. Kiernan, A.V. Kirshnan, C.S. Lin, D. Burkke, S.F. Berkovic, Mutation in the Na+ channel subunit SCN1B produces paradoxical changes in peripheral nerve excitability, Brain 128 (2005) 1841–1846.
[25] C. Aizenmann, D.J. Linden, Rapid, synaptically driven increases in the intrinsic excitability of cerebellar nuclear neurons, Nat. Neurosci. 3 (2000) 109–111.
[26] S. Armano, P. Rossi, V. Taglietti, E. D'Angelo, Long-term potentiation of intrinsic excitability at the mossy fiber-granule cell synapse of rat cerebellum, J. Neurosci. 20 (2000) 5208–5216.
[27] N.S. Desai, L. Rutherford, G.G. Turrigiano, Plasticity in the intrinsic excitability of cortical pyramidal neurons, Nat. Neurosci. 2 (1999) 515–520.
[28] M. Zhang, F. Hung, Y. Zhu, Z. Xie, J. Wang, Calcium signal-dependent plasticity of neuronal excitability developed postnatally, J. Neurobiol. 61 (2004) 277–287.
[29] T.F. Freund, G. Buzsaki, Interneurons of the hippocampus, Hippocampus 6 (1996) 347–470.
[30] A. Sik, A. Ylinen, M. Penttonen, G. Buzsaki, Inhibitory CA1-CA3-hilar region feedback in the hippocampus, Science 265 (1994) 1722–1724.
[31] A.G. Carter, W.G. Regehr, Quantal events shape cerebellar interneuron firing, Nat. Neurosci. 5 (2002) 1309–1318.
[32] R. Azous, C.M. Gray, Dynamic spike threshold reveals a mechanism for synaptic coincidence detection in cortical neurons in vivo, Proc. Natl. Acad. Sci. USA 97 (2000) 8110–8115.
[33] A.R. Cantrell, W.A. Catterall, Neuromodulation of Na+ channels: an unexpected form of cellular plasticity, Nat. Rev. Neurosci. 2 (2001) 397–407.
[34] C.M. Colbert, E. Pan, Ion channel properties underlying axonal action potential initiation in pyramidal neurons, Nat. Neurosci. 5 (2002) 533–538.